JOURNAL OF SPACECRAFT AND ROCKETS
Vol. 42, No. 5, September–October 2005

Oxidation Behavior of Siliconcarbide-Based Materials by Using New Probe Techniques

G. Herdrich,* M. Fertig,† S. Löhle,‡ S. Pidan,‡ and M. Auweter-Kurtz§
University of Stuttgart, 70550 Stuttgart, Germany
and
T. Laux¶
DLR, German Aerospace Center, Stuttgart, 70503 Stuttgart, Germany

Hysteresis of passive to active and active to passive transition of SiC oxidation behavior has been investigated theoretically, numerically, and experimentally. Theoretical and experimental investigations show a strong interaction between transition and catalysis. Dependence on plasma composition is shown. A recently developed reaction model has been implemented in the advanced nonequilibrium Navier–Stokes code URANUS. Results are presented for the highly dissociated flow around the MIRKA capsule. In this case, radiation adiabatic surface temperatures have been found to be 120 K higher for active oxidation conditions as compared to passive oxidation conditions. To investigate transition behavior in detail, various new probe measurement techniques have been developed. Important additional observations have been made in chemical nonequilibrium. Within plasma wind-tunnel testing, a sudden temperature increase of up to 400 K was found with the transition from passive to active oxidation. Theoretical and numerical predictions show good qualitative and quantitative agreement with experimental results.

Nomenclature

A	=	section area
c	=	heat capacity
M_a	=	Mach number
p	=	pressure
q	=	integral heat flux
s	=	thickness
T	=	temperature
t	=	time
V	=	volume
v	=	velocity
x	=	distance from plasma generator outlet plane
γ	=	ratio of heat capacities
ΔH	=	reaction enthalpy
δ	=	boundary-layer thickness
ε	=	emissivity
ρ	=	density
Φ	=	angle

Subscripts

amb	=	ambient
(g)	=	gaseous
in	=	related to temperature of water coming into cooling system
out	=	related to temperature of water leaving cooling system
(s)	=	solid
tot	=	total
W	=	related to wall
1	=	situation before shock
2	=	situation behind shock

Presented as Paper 2004-2173 at the AIAA 37th Thermophysics Conference, Portland, OR, 28 June–1 July 2004; received 16 July 2004; revision received 9 December 2004; accepted for publication 17 December 2004.

*Research Engineer, Institut für Raumfahrtsysteme, Pfaffenwaldring 31; herdrich@irs.uni-stuttgart.de. Member AIAA.
†Research Engineer, Institut für Raumfahrtsysteme, Pfaffenwaldring 31. Member AIAA.
‡Research Engineer, Institut für Raumfahrtsysteme, Pfaffenwaldring 31.
§Professor, Institut für Raumfahrtsysteme, Pfaffenwaldring 31. Associate Fellow AIAA.
¶Research Engineer, P.O. Box 800320, Institut für Bauweisen-und Konstruktionsforschung. Member AIAA.

Introduction

REENTRY flight experiments have already been performed in which SiC-based thermal protection systems (TPS) were used with the emphasis to investigate their reusability.[1–4] It was shown that C/C–SiC, which is carbon fiber-reinforced SiC, is able to withstand severe thermal loads even at temperatures of about 2500 K (Ref. 2). However, such loads are extraordinary and represent an adversity of the desired reusability of the TPS. Additionally, for typical reentry vehicles, high lift over drag ratios are aimed for to realize both controllability and high crossrange. Therefore, subsystems such as flaps and rudders are required in combination with an appropriate aerodynamic shape, which is usually associated with narrow radii or sharp edges. Moreover, the connections of TPS segments and the interfaces between substructures lead to steps or gaps. With the occurrence of the so-called active oxidation regime, which is ongoing with an evident temperature jump at the passive to active oxidation transition (PAT), substantial mass loss rates arise that have to be taken into account, because they can be mission critical otherwise. Therefore, at the Institut für Raumfahrtsystem (IRS), extensive campaigns were performed to investigate the PAT.[5] These investigations were supplemented by additional work in the field of plasma–surface interaction[6] with in-flight measurements.[1]

In principal, chemical reactions of SiC with oxygen lead to the formation of SiO, SiO_2, CO, and CO_2, the latter of which is of negligible importance at the expected temperatures. Both SiO and CO are gaseous at those temperatures, thereby leading to erosion and a rapid material loss. In contrast, SiO_2 is liquid or solid at the lower temperatures. It forms a layer on top of the SiC and acts as a diffusion barrier, which can be considered a self-protection mechanism because oxygen flux to the surface is hindered. Hence, mass loss rate under these so-called passive oxidation conditions is much lower. At higher temperatures and lower oxygen pressure, an SiO_2 layer is removed and SiO formation becomes more likely. This process is called active oxidation. Figure 1 shows the trajectories of the recent reentry mission EXPERT (and X-38) in comparison to the PAT regime based on the equilibrium model of Heuer and Lou.[7] As

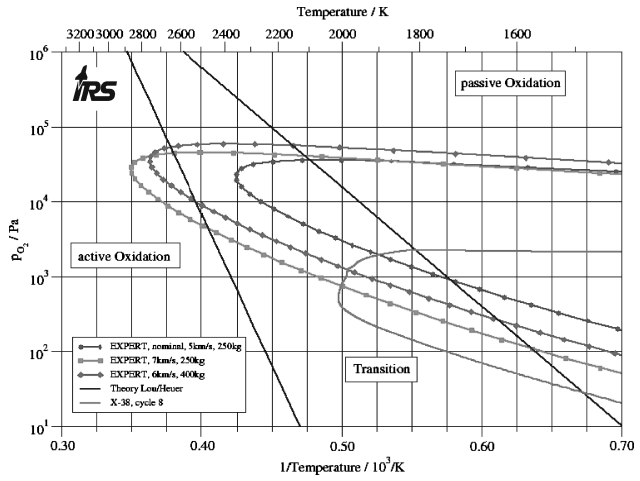

Fig. 1 Nominal entry trajectories of EXPERT[4] and X-38 (Cycle8) related to active, passive, and transitional oxidation regimes (model of Heuer and Lou[7]).

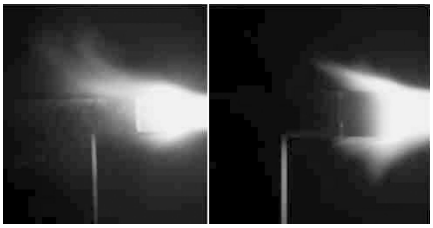

Fig. 2 PAT using plasma source IPG3, pure oxygen plasma.

can be seen, active oxidation may occur at the TPS of both vehicles. However, equilibrium models are not able to predict the transition during reentry properly because the boundary layer around vehicles is characterized by chemical nonequilibrium at high altitudes.

The temperature increase that appears with the PAT is associated with an increase of thermal load that can cause mission failure. Within the German research program Ausgewählte Technologien für Zukünftige Raumtransportsystem-Anwendungen (ASTRA), IRS investigates basic pressureless sintered siliconcarbide (SSiC) materials and C/C-SiC composites [German Aerospace Center, Stuttgart, Germany (DLR-S) and MAN Technologie AG (MAN-T)] using pure oxygen and air plasmas to identify the involved reaction schemes. This is of very high importance, because previously performed investigations imply that a decisive share of the energy seen by the TPS during active oxidation could be contributed by nitrogen reactions that are ongoing with the oxidation regime.[8] Test campaigns in oxygen atmospheres have been performed using the inductively heated plasma wind tunnel 3 (PWK3). This facility offers the advantage to be operated even with pure reactive gases such as oxygen[9,10] leading to a significant simplification of the reaction regimes. This is of importance because Hilfer,[5] for example, investigated more than 170 potential reactions in his work, which he reduced to six essential reactions for SiC. Laux investigated the oxidation behavior of sintered silicon carbide experimentally, with theoretical analysis for air and for pure oxygen plasma, from which he found out that the temperature jump as well as the erosion rate are smaller than in air plasma, leading to the conclusion that nitrogen, especially atomic nitrogen, plays an important role in explaining the sudden temperature increase.[11] However, it is found that all measured transitions lie within the regime predicted by Heuer and Lou.[7] Figure 2 shows an SSiC material sample in PWK3 (oxygen plasma) in the active oxidation regime (Fig. 2a) and the passive oxidation regime (Fig. 2b) as investigated by Laux.[11]

The change in plasma brightness (on the left-hand side of Fig. 2) which is accompanied with green color, can be explained by the creation of gaseous molecules such as CO and C_2 in which the carbon is contributed as erosive product by the material sample. Simultaneously, temperature rises by around 200 K, and the erosion increases by orders of magnitude.

The campaigns and measurements are combined with nonintrusive techniques such as laser-induced fluorescence (LIF). In addition, new probe technologies have been developed at IRS to characterize the oxidation regimes. One of them is a double probe with different materials at an identical plasma condition. In fact, this probe has been developed for the measurement of recombination coefficients from local heat flux measurements.[12] However, simulations using the nonequilibrium URANUS code indicate that catalysis plays an important role for the consideration of PAT and active to passive transition (APT). Fertig et al. introduced in this flow simulation code a detailed surface reaction model that accounts for catalytic and oxidative reactions at the surface resulting in different transition mechanisms from passive to active oxidation for SiC and an evident influence of the catalycity.[8]

To extend the knowledge of the chemical behavior, especially at these transition condition, a spectroscopic probe has been developed. In the present paper, the measured spectra in the boundary layer in front of the material sample and first measurements are presented. First a brief introduction in relevant surface reactions is given and comparisons to more difficult computations are made. The used probe technique for the investigation of catalytic effects on the PAT together with numerical results is shown as well.

Surface Reactions

Although more than 170 different reactions are possible in the Si–C–N–O system, most phenomena responsible for reentry vehicle heating can be explained by a small subset. In the reactions of SiC with oxygen at the surface of a reentry vehicle, either gaseous SiO,

$$\mathrm{SiC(s)} + \mathrm{O_2} \leftrightarrows \mathrm{SiO(g)} + \mathrm{CO}, \qquad \Delta H_f^0 = -139\ \mathrm{kJ\ mole^{-1}} \quad (1)$$

$$\mathrm{SiC(s)} + 2\mathrm{O} \leftrightarrows \mathrm{SiO(g)} + \mathrm{CO}, \qquad \Delta H_f^0 = -638\ \mathrm{kJ\ mole^{-1}} \quad (2)$$

or SiO_2, which may be either solid or liquid,

$$\mathrm{SiC(s)} + \tfrac{3}{2}\mathrm{O_2} \leftrightarrows \mathrm{SiO_2(s)} + \mathrm{CO}, \qquad \Delta H_f^0 = -950\ \mathrm{kJ\ mole^{-1}} \quad (3)$$

$$\mathrm{SiC(s)} + 3\mathrm{O} \leftrightarrows \mathrm{SiO_2(s)} + \mathrm{CO}, \qquad \Delta H_f^0 = -1697\ \mathrm{kJ\ mole^{-1}} \quad (4)$$

are formed together with gaseous CO. In principle, passive oxidation, that is, formation of an SiO_2 layer, could lead to a material gain because two oxygen atoms have higher mass than one carbon atom. However, this is only the case until a stationary-layer thickness is reached. Under reentry conditions, the stationary state is typically reached within a few seconds. Afterward, the formation of SiO leads to surface erosion.

Fundamental work on surface oxidation has been performed by Wagner[13] and Turkdogan et al.[14] Their models have been discussed in the past to explain the conditions that lead to PAT of SiC. Wagner investigates two possible states: either the oxidation with Si or the reactions with an already passive oxidized surface, that is, an SiO_2-layer. Depending on the oxygen pressure, he can calculate the conditions for PAT in steady-state conditions. Turkdogan also investigated theoretically the Si surface, but he already introduced a possible vaporization of the Si from the surface with adjacent reactions with oxygen. He introduces a possible loss of vaporized Si due to a velocity parallel to the surface that can result from an axial flow velocity. Therefore, the model of Turkdogan can be understood as a model including a gas flow. The simplified explanations given by Wagner and Turkdogan both do not consider bubble formation, which is one reaction mode leading to fast surface erosion.[5] They both explain the conditions when PAT occurs, but do not explain an ongoing temperature increase.

In the reaction environments considered in this paper, active oxidation occurs if an SiO_2 layer is neither present nor formed. Transfer of Wagner's model to SiC oxidation indicates that the chemical equilibrium of SiO depending on the oxygen partial pressure is responsible for PAT. Hence, two reactions, that is,

$$\mathrm{SiO_2(s)} \leftrightarrows \mathrm{SiO(g)} + \tfrac{1}{2}\mathrm{O_2}, \qquad \Delta H_f^0 = 810\ \mathrm{kJ\ mole^{-1}} \quad (5)$$

$$\mathrm{SiO_2(s)} \leftrightarrows \mathrm{SiO(g)} + \mathrm{O}, \qquad \Delta H_f^0 = 1059\ \mathrm{kJ\ mole^{-1}} \quad (6)$$

for molecular and atomic oxygen may be formulated. Both reactions are endothermic and produce gaseous species. It follows from both reactions that SiO formation velocity increases with rising temperature and decreasing oxygen pressure. Because formation of SiO from SiC is exothermal, surface heating should be higher after transition. In measurements with conditions close to chemical equilibrium, no such increase has been observed so far. Because surface emission and absorption coefficients change during APT, measurement may be impossible under equilibrium conditions, especially if changes are small. To explain the temperature increase of about 200 K, more sophisticated models have to be introduced. Fertig et al.,[8] for example, included catalytic reactions while solving the flow situation numerically. One of the major problems in PAT prediction is that SiO_2 formation under passive oxidation conditions takes place at the interface between SiO_2 and SiC (Ref. 15), whereas SiO_2 decomposition proceeds at the SiO_2–gas interface or anywhere within the SiO_2 layer. Hence, PAT is a function not only of diffusion characteristics in the gas but also of diffusion characteristics in the SiO_2 layer. Moreover, transition at oxygen pressures of about 10^5 Pa arises at temperatures above 2000 K. Hence, it is in question whether measurements of PAT in chemical equilibrium are possible at all. The situation becomes more complicated in the case of chemical nonequilibrium because catalytic phenomena arise additionally.[16]

Turkdogan et al. developed models to explain nonequilibrium effects caused by, for example, gas flow. Gas flow removes reaction products from the reaction zone but transports reaction educts to the reaction zone. Because of a higher oxygen fraction, the formation of SiO_2, but also SiO, speeds up. Removal of SiO, on the other hand, speeds up SiO_2 decomposition such that transition might be expected at lower temperature. The model of Turkdogan et al. determines reaction rates depending on a combination of sublimation and diffusion. Transfer of their model to the PAT of SiC would state that Si sublimates at the surface and moves into gas phase such that the gas close to the surface would consist of Si vapor. Oxygen from the gas diffusing toward the surface reacts with the Si vapor, forming SiO and SiO_2. Hence, a gas flow would remove the Si vapor such that erosion speeds up. This model, however, has multiple deficiencies: The SiO_2 layer would grow at the outer SiO_2 surface due to condensation, which is in contrast to measurements.[15] SiC is stable up to about 2600 K in an inert atmosphere even with gas flow. The fraction of Si to C should change, which is not the case. Under reentry conditions in which gas temperature rises from values of about 2000 K at the surface to about 7000 K at the edge of the boundary layer, no formation would be possible. However, SiO_2-layer formation is possible under such conditions as well.

However, Wagner's model states that PAT is associated with a much lower SiO partial pressure than the reversal process, that is, APT. Hence, Wagner states that transition characteristics are associated with a hysteresis concerning SiO and oxygen partial pressures. The observation that transition from active to passive oxidation is also possible in rarefied gas flows in which the SiO partial pressure is about zero[17] indicates that neither Wagner's nor the model of Turkdogan et al. is applicable for the prediction of APT under reentry conditions.

Moreover, Wagner's model is not able to explain the value of the sudden temperature rise in nonequilibrium air with PAT. Although a change from the endothermic decomposition of SiO_2 to a rapid exothermic erosion of SiC due to SiO formation allows for an explanation of the temperature jump of about 200 K in pure oxygen plasma, it is not sufficient to explain a surface temperature rise of about 400 K as measured in air. Catalytic effects and heterogeneous kinetics have to be considered in addition, as shown by Fertig et al.[8] SiO_2 is of medium-to-low catalytic activity with respect to oxygen and nitrogen at temperatures of transition. SiC, on the other hand, has a high catalytic activity under these conditions for nitrogen recombination.[16] Hence, PAT in air increases not only heating due to SiC erosion increases, but also catalytic heating due to atomic nitrogen recombination. This observation is confirmed by the analysis of Laux who performed tests with varying oxygen mass flow with pure oxygen tests, leading to the conclusion that the higher temperature increase in air plasma can be a result of atomic nitrogen recombination reactions.[11]

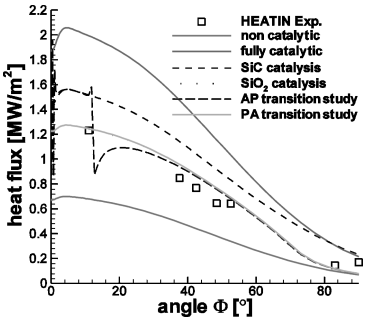

Fig. 3 Axisymmetric URANUS nonequilibrium Navier–Stokes simulation for MIRKA peak heating conditions with multiple gas–surface interaction models applied.[19]

Results

The heterogeneous surface model proposed in Ref. 8 has been employed for the simulation of the reentry loads of the Mikro-Rückkehrkapsel (MIRKA) vehicle.[18]

Figure 3 shows surface heat loads computed with the axisymmetric URANUS nonequilibrium Navier–Stokes code at peak heating conditions in about 60 km of altitude performed within the German ASTRA program.[19] Free flow conditions in all simulations are $v_\infty = 6626.3\ \mathrm{m \cdot s^{-1}}$ at a density of $\rho_\infty = 5.043 \times 10^{-4}\ \mathrm{kg \cdot m^{-3}}$ with an ambient pressure of $\rho_\infty = 37.88$ Pa. SiC and SiO_2 catalysis models and the surface reaction model proposed in Ref. 8, which is labeled AP transition study and PA transition study, with radiation equilibrium surface have been applied. For reference, results of noncatalytic and fully catalytic boundary conditions are shown. To investigate whether PAT oxidation was possible for MIRKA's flight conditions, results obtained with the SiO_2 catalysis model have been used as an initial solution. For the APT study, the surface temperature was set to 2300 K initially. The hysteresis of the results shows that MIRKA flight was in the transition regime between active and passive oxidation. From the agreement of the heat fluxes computed for the PA transition study with the SiO_2 catalysis model, it follows that chemical energy release at the surface is dominated by catalytic reactions on the protective SiO_2 layer. The agreement of the SiC catalysis results where surface erosion is neglected with the AP transition study in the stagnation area show the domination of catalytic processes under active oxidation conditions as well. However, this domination of catalytic heating, which is significant for MIRKA, is not expected to be a general feature. For the European Experimental Re-Entry Testbed (EXPERT) reentry flight, for example, about one-third of the total heat flux to the surface might arise due to active oxidation.

Probe Techniques

In the following text, the probe technique used to investigate the PAT is described. First, the well-established probes such as steady-state heat flux and a pitot pressure probe are presented because they are used to investigate the plasma flow itself. Afterward, the newly developed probe technique is explained in more detail with special focus on the applicability to investigate catalytic and oxidative behavior.

The steady-state heat flux is measured on an insert that can easily be changed and can be made out of different materials, normally copper because of its high catalycity. For the stationary case the flow rate through the insert $\dot{V}$ and the temperature difference of the incoming and outgoing water ($T_{\mathrm{out}} - T_{\mathrm{in}}$) are measured, the latter by electrically insulated and shielded resistance thermometers Pt100. The heat flux per unit area is then given by

$$\dot{q} = c_{p,w} \rho_W \dot{V}_W (T_{\mathrm{out}} - T_{\mathrm{in}})/A \tag{7}$$

where $c_{p,w}$ is the heat capacity of water, ρ_W the water density, and A the surface area of the probe exposed to the plasma (Fig. 4).

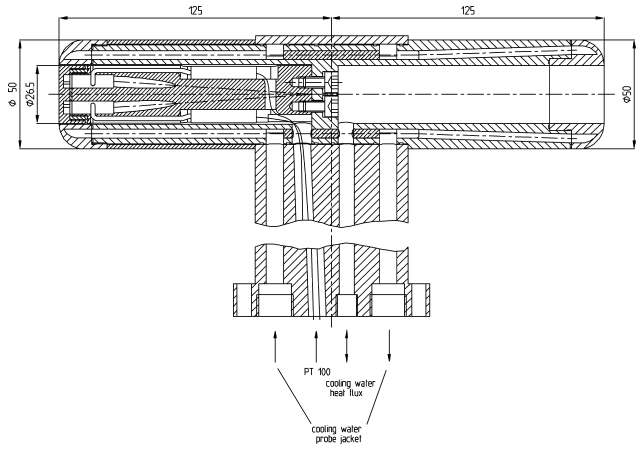

Fig. 4 Steady-state heat flux and pitot pressure double probe.

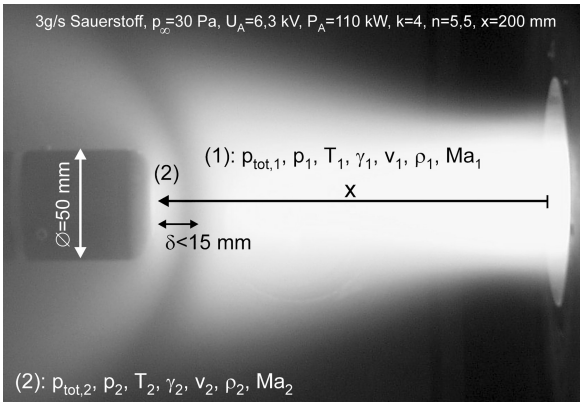

Fig. 5 Supersonic flow condition in PWK3 (IPG3) with notation for flow parameters and axis definition.

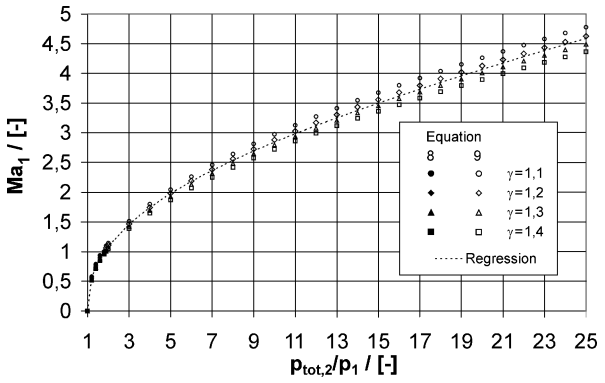

Fig. 6 Ma_1 depending on pressure ratio $p_{tot,2}/p_1$.

The pitot pressure enables statements on the flow condition, in particular on the Mach number of the plasma flow, by using (subsonic)

$$1 + [(\gamma - 1)/2]M_{a1}^2 = (p_{\text{tot}}/p_{\text{amb}})^{(\gamma-1)/\gamma} \tag{8}$$

For the supersonic case, we have to use

$$\frac{[(\gamma + 1)/2]M_{a1}^2}{\left\{[2\gamma/(\gamma + 1)]M_{a1}^2 - [(\gamma - 1)/(\gamma + 1)]\right\}^{1/\gamma}} = \left(\frac{p_{\text{tot}}}{p_{\text{amb}}}\right)^{(\gamma-1)/\gamma} \tag{9}$$

where γ is the adiabatic coefficient and M_{a1} is the Mach number. The notations are shown in Fig. 5 ($p_1 \approx p_{\text{amb}}$). Both equations assume constant heat capacities. The static pressure is assumed to be the ambient pressure in the vacuum chamber. In Fig. 6, the resulting Mach numbers are illustrated. The full symbols show the interval calculated using Eq. (10), whereas the empty symbols were calculated with Eq. (11). Here, γ is varied between 1.1 and 1.4.

Newly Developed Probe Techniques

Catalysis Probe

To enhance the measurement technique toward a better heat flux estimation of the real heat shield material sample, a new probe with two pyrometric devices has been developed. The new double probe for both material and catalytic investigations in the plasma streams has recently been developed and qualified at IRS. With the double probe, it is possible to investigate two materials simultaneously under the same plasma condition. It is equipped with two miniaturized pyrometers (Pyrex™) integrated in the measuring heads using the standard European sample geometry (Fig. 6). Each pyrometric device records the surface temperature of the rear side of the investigated material sample. The probe allows for transient and steady-state heat flux measurements, whereas the steady-state temperature of the investigated sample can reach the value of about 2200°C.

Radiation with a 630-nm wavelength from the sample's rear side is fed through the optical path of the Pyrex sensor to the electronic box where the photodiodes are installed (Fig. 7). The optical path consists of one silicon carbide tube, a lens system, and a bundled fiber optic cable. The electronic box contains two photodiodes and the electronic components required for the photodiode's signal treatment. The output signal of the electronic box is a RS422 data word. The temperature measurement rate is 10 Hz for each channel. Because of the geometric shape of the sensor head and silicon carbide tube, the measured temperature values do not depend on the surface emissivity of the material. The geometrically formed cavity leads to an effective emissivity value of almost one.

With the measured temperature history data, the heat flux history on tested material samples can be calculated employing the thin-wall method. Because of the high-temperature insulation behind the material sample, the rear side of the sample can be assumed adiabatic. Because the ambient temperature is quite low, the ambient radiation can be neglected. When the one-dimensional theory of heat flux propagation is considered, the heat flux on the material sample can be calculated according to

$$\dot{q}_{\text{sample}} \approx \varepsilon\sigma T_w^4(t) + c_p \rho s \frac{\mathrm{d}T_w(t)}{\mathrm{d}t} \tag{10}$$

With the probe, both the determination of material emissivity and recombination coefficients is possible in situ (Fig. 8).

Spectrometer Probe

Although emissions spectroscopic measurements are already known at IRS, a new probe technique including this measurement possibility is needed because of two reasons: From the measurements using a spectrometer outside of the vacuum chamber, it is impossible to get a line of sight parallel to the plasma flow. The second

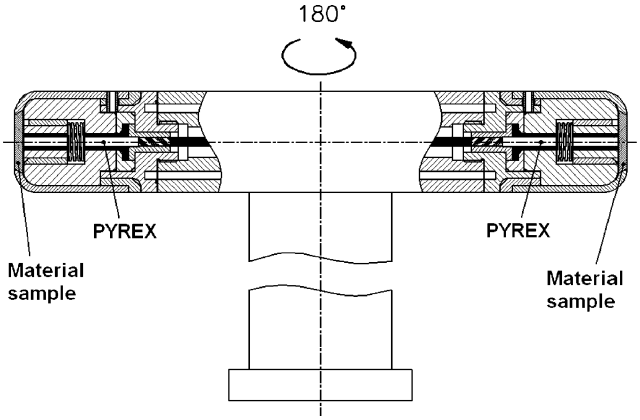

Fig. 7 Material double probe (catalysis probe) with mini-pyrometers (Pyrex).

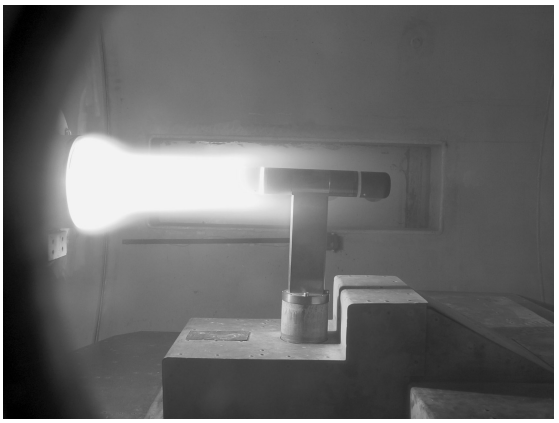

Fig. 8 Material double probe in operation (PWK2, RD5).

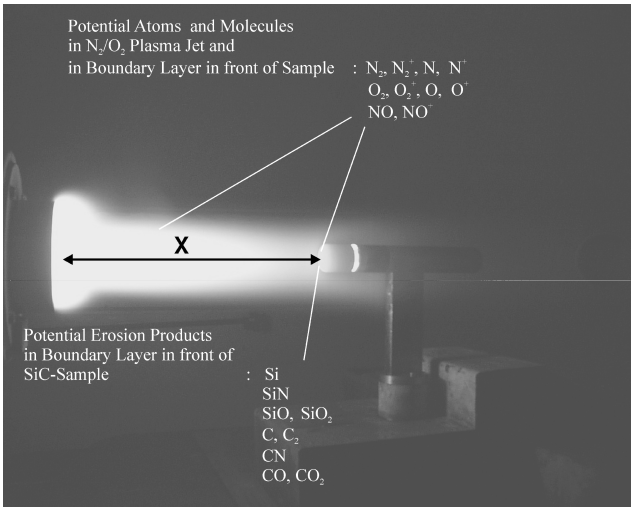

Fig. 9 Species expected in plasma/boundary layer using SiC-based material sample in air plasma; magnetoplasmadynamically driven PWK2-RD5, *x* position shown.

reason is that future flight experiments will need a setup consisting of the main parts of this new probe. Hence, it is understood to be a first step to the new flight experiment. The design of the so-called spectrometer probe is based on the experiences made in the past, for example, with Pyrex[1] and the IRS radiometer probe used for the measurement of the radiative heat flux.[20] However, the measurement task is even more ambitious in this case because emission spectra in a wavelength range between 200 and 880 nm are measured. This is achieved by application of a miniaturized spectrometer (Avantes S2000) together with an optical access, that is, a bore hole through the material sample. Correspondingly, the species, that is, both the species from the reactive plasma flow and the erosion products in the boundary layer in front of the material sample, shall be measured. Figure 9 shows the expected species based on the expected air plasma species and corresponding erosion products, for example, Eqs. (1–6). The setup has to be thermally resistive and possess active cooling of the optical path, and the material sample must be prevented.

When both the design and the approval of the probe during plasma tests are considered, the probe can be considered as a laboratory model for EXPERT's flight experiment RESPECT.[21]

The setup is shown in Fig. 10. The material sample (in these investigations, pressureless sintered SiC) itself is equipped with a hole to allow for the needed optical access to the boundary layer. Behind the sample, an SiC tube that serves as an optical path is placed. The setup, in particular the sample and tube, are pressed together using a spring system. With this system, the setup becomes more flexible, for example, for the integration of samples with different hole di-

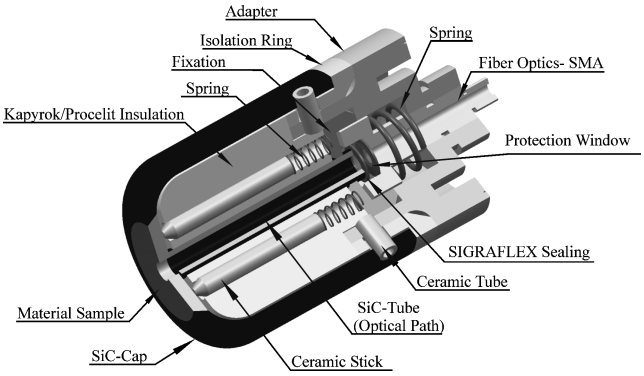

Fig. 10 Design of IRS spectrometer probe.

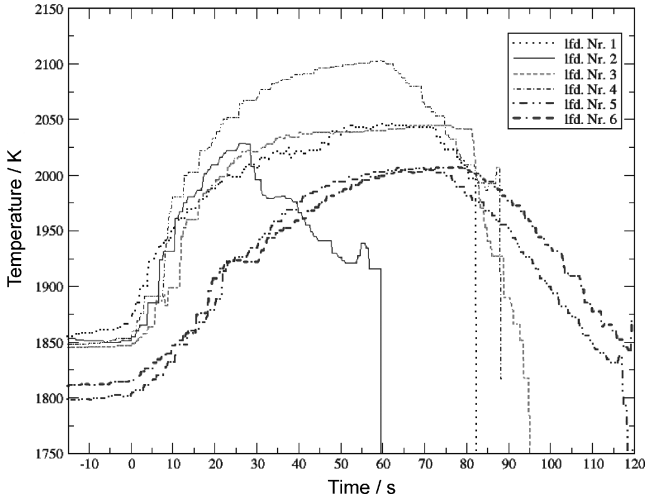

Fig. 11 Heat flux history on different materials investigated with double probe.

ameters. The fiber-optic system that transmits the detected radiation to the spectrometer housing is mounted in an adapter. This adapter is separated from the hot structures by an insulation ring. Between the adapter and SiC tube, a protection window is mounted. This window is sealed by using two flexible graphite foil (SIGRAFLEX) sealings. The modular design enables the integration of filters. The material sample and the SiC tube are integrated in an SiC cap and surrounded by an Al_2O_3-based insulation. The probe geometry corresponds to the European standard design of plasma wind-tunnel probes (diameter of 50 mm).

Measurement Results

The newly developed probes have both been used to underline the commonly known phenomena of PAT. In the following section, results from conventional measurements are presented to introduce the problems that can probably be solved using the new probe technique. These results are added after this more general introduction into the measurements made at IRS.

Erosion Behavior and Temperature Increase

Catalytic properties of the materials used have been compared qualitatively with results from experiments in the plasma wind tunnel PWK2. A quantitative comparison of the catalytic activities of the investigated materials was done with the heat flux and plasma characteristic values measurements performed in the plasma wind tunnel PWK3. (See also Ref. 12.) Measured values of the heat fluxes on the different materials obtained in the plasma wind tunnel PWK2 allow the qualitative comparison of the catalytic behavior of the investigated materials. Figure 11 shows the heat flux histories on four materials, namely SSiC, Spinel, C/C–SiC with CVD–SiC coating (DLR, German Aerospace Research Institute, Stuttgart), and C/C–SiC with yttrium silicate coating (DLR-Stuttgart). These

measurements have been performed in the PWK2 with the plasma generator RD5. A description of the magnetoplasmadynamically driven PWK2 can be found in Ref. 22. The condition was at an ambient pressure of 490-Pa using a current of 1070 A with a voltage of 91.3 V. The plasma generator RD5 was operated with 6.14 g/s nitrogen, 1.86 g/s oxygen, and 0.3 g/s argon.

As expected, the results show approximately equal hear fluxes on the SSiC and C/C–SiC with CVD–SiC coating. The heat flux on Spinel is clearly lower than that on SSiC, whereas the heat flux on the C/C–SiC with yttrium silicate coating is higher compared to the one on SiC. This indicates that Spinel is less catalytic vs air as silicon carbide; yttrium silicate is shown to be more catalytic vs air than SSiC.

However, during the tests, the steady-state temperature of the Spinel sample was higher than the steady-state temperature of the SSiC sample, whereas the heat flux on Spinel was much lower than that on SSiC. This difference in temperature is caused by the difference in total emissivity of both materials. In this temperature range, Spinel has a total emissivity value of about 0.4, whereas the SSiC's value is about 0.8. Hence, the total surface emissivity is a very important factor for correct material investigation. Although low heat fluxes are measured, caused for example, by low catalytic activities of the material, the surface temperature can be quite high because of the low emissivity value.

Figure 12 shows a typical PAT under the same plasma generator condition. The transition occurs when the probe is moved slightly in direction of the plasma generator's outlet, such that the temperature of the probe reaches the temperature where active oxidation may occur. Reaching $x = 280$ mm, where total pressure $p_{\text{tot}} = 760$ Pa as measured with the pitot pressure probe, shown in Fig. 4, the temperature increases. This temperature increase shows a typical relaxation behavior. After almost 100 s, a sudden temperature increase of roughly 380 K occurs. Simultaneously, the erosion rate increases by more than one order of magnitude from 2.97 to 54.48 kg/(m^2 · h) (SSiC), as theoretically analyzed in the "Surface Reactions" section. A similar behavior can be observed for the tested CVD coated C/C–SiC material from DLR Stuttgart (Table 1). Experimentally, the erosion rate is measured by balancing the probe before and after test together with the time the probe replaced at a certain oxidation state.

Table 1 Erosion rate and temperature data

Condition	T/K	Erosion rate, kg/(m^2 · h) (time in plasma jet/s)
Passive SSiC	1652	2.9734 (600)
Passive C/C–SiC	1647	3.9641 (172)
Active SSiC	1683 (start) 2060 (maximal)	54.4833 (182)
Active C/C–SiC	1708 (start) 2015 (maximal)	39.1113 (181)

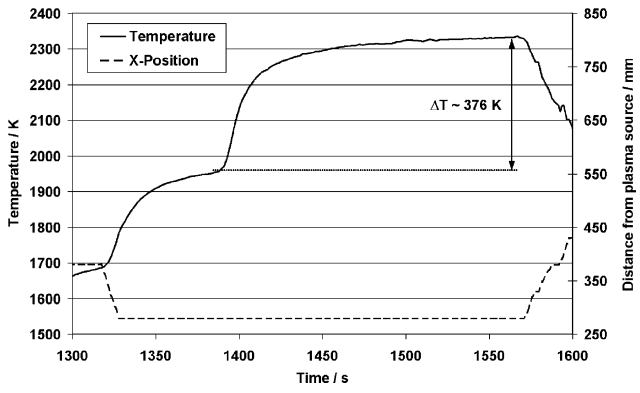

Fig. 12 SSiC transition from passive to active oxidation in PWK1 air plasma.

Figure 13 shows a hysteresis experiment: Here, the sample was stepwise moved (back) to the nominal active condition ($x = 288$ mm). The presented temperature increase, however, does not represent a steady-state value because the sample was moved back stepwise to a nominal passive position at $x = 338$ mm. Here, it can be observed that it takes more than 4 min before APT is finalized. For a reentry flight, this situation is very critical. If active oxidation occurs, the vehicle may rest again for a longer time in the critical active oxidation, even when active oxidation conditions (Fig. 1) are not given anymore. An explanation for this observation is that the surface temperature decreases because the greater distance to the nozzle exit takes time, whereas the chemistry again has a longer delay. Theoretical studies of this material behavior have not been performed so far.

In Fig. 14, PAT in pure oxygen plasmas using the inductively heated plasma wind tunnel PWK3 for different ambient pressures between 40 and 3000 Pa are shown. Major differences to PAT in air plasma are the lower temperature differences ΔT that are between 150 and 250 K and the higher erosion rates that are between 117 and 167 kg/m^2/h.

Both observations can be generalized. This is in good agreement with predictions based on the surface reaction model implemented in the URANUS code. (see Results section). Correspondingly, the additional energy release accompanying the active oxidation in air plasmas can be explained by nitrogen recombination. This result is confirmed by the considerations of Laux, who measured PAT both in air plasma using IRS arcjet-driven facilities and the inductively driven PWK3 (Ref. 11).

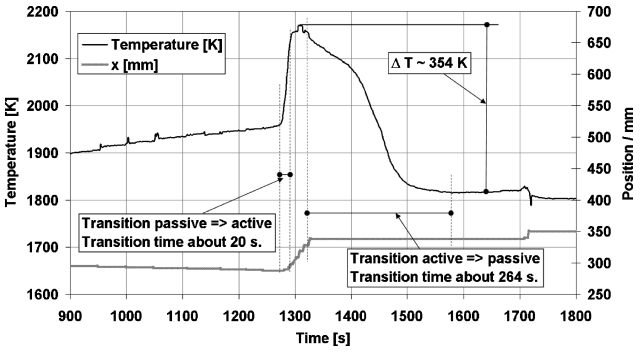

Fig. 13 PAT and APT of SSiC in PWK1-MPD air plasma, hysteresis effect.

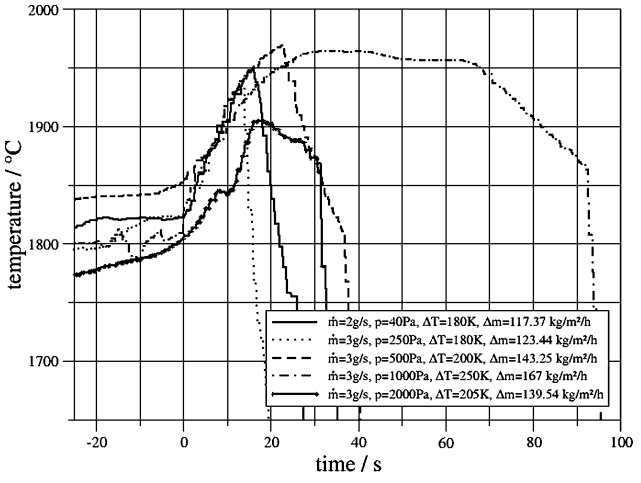

Fig. 14 PAT in pure oxygen plasma (inductively heated PWK3).

Plasma Species

For more detailed experimental investigation of the plasma species in the boundary layer, spectroscopic measurements are required. In Fig. 15, an exemplary result using the spectroscopic probe in PWK2 (RD5) is shown.

Apart from species resulting from the air plasma and plasma generation processes, for example, N^+, species such as Si, SiN, and CN can be seen (Fig. 9). In fact, the change of the spectra themselves with PAT is rather low. However, when Fig. 16, which is a zoomed interval of the upper part of Fig. 15, is considered, it can be seen that Si increases with PAT. This corresponds very well to the theoretical approaches that assume Si gas near the surface, as well as with mass spectroscopic measurements by Dabala.[6] Almost all of the mentioned erosion products (Fig. 4) are detected for both oxidation regimes. Nevertheless, a change of the signal is not detected for most of the erosion products, which can also be due to resolution effects of the spectrometer. The Si signal and, marginally, the CN signal at 385 nm increase with PAT. For some of the species, for example, SiO and SiN, this observation may be explained as follows: In particular, these species are not that chemically stable, and it is evident that the produced SiO experiences a diffusion process toward the hot boundary layer, leading to its dissociation. Additionally, it is possible that these erosion products are not highly excited, such that a possible emission can be seen. In this manner, the increase of the Si could be an indirect measurement of Si-related erosion products dissociated in the hot zone of the boundary layer in front of the SSiC material sample.

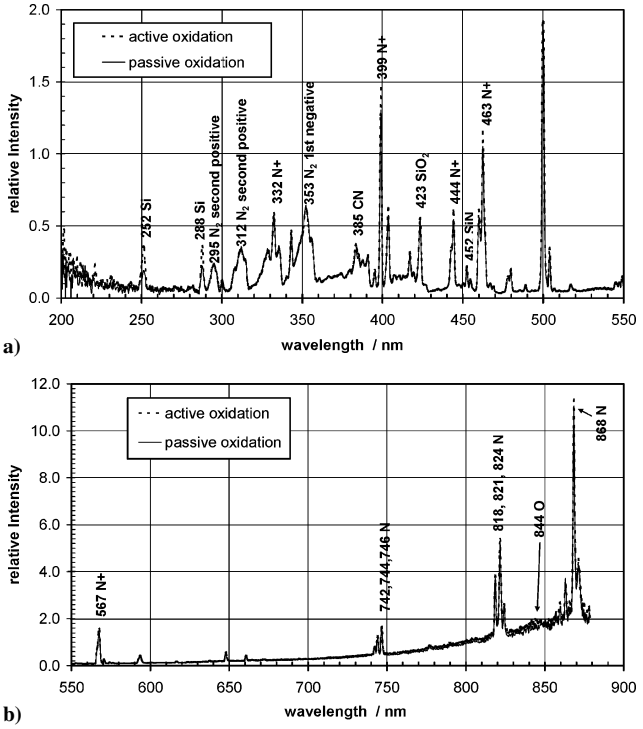

Fig. 15 Boundary-layer spectra, PAT: comparison of situation under passive oxidation and active oxidation.

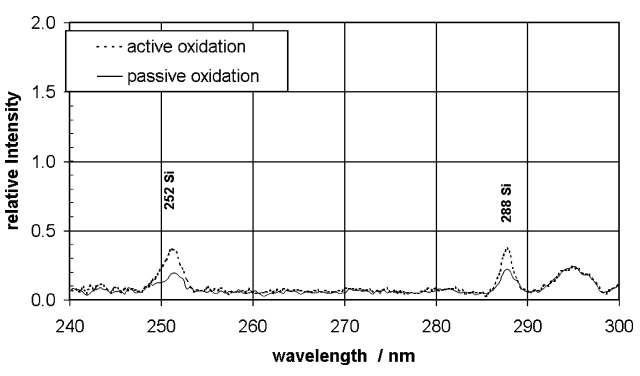

Fig. 16 Zoom of PAT spectrum (Fig. 15), increase of Si radiation.

The present investigation belongs to the initial measurement campaigns being performed with the new spectroscopic probe. It has to be emphasized that further analysis and experiments are required for a better understanding of the situation. For example, with the exception of CN, carbon containing species could hardly be identified. From the systematic point of view, two approaches have to be performed. First, disturbing radiation of the species originating from the plasma generation process could be reduced by slightly turning the probe around its axis. However, it must investigated whether active oxidation can still be triggered in this case. The second approach is performing PAT experiments in the inductively driven plasma wind tunnel PWK3 using pure oxygen to reduce the amount of different species in general and to underline the PAT behavior as shown in Fig. 12. This may simplify the analysis of species, for example, in the wavelength intervals shown in Fig. 15. Finally, an appropriate wavelength filter can improve the measurements for certain species.

Recommendations

Active oxidation may occur during the flight of EXPERT. In particular, the trajectories with entry velocities of 6.9 km/s (250 kg) and 6 km/s (400 kg) seem to have this potential. This has to be investigated more in detail by means of testing and numerical analysis. However, all of the trajectories are in the transition area shown in Fig. 1, although the model used for the determination of the transition zone in Fig. 1 has been calculated employing the equilibrium model of Heuer and Lou.[7] Therefore, nonequilibrium effects due to significant heterogeneous processes at the surface are not considered, but have to be accounted for as shown exemplarily for the MIRKA capsule by Fertig (Fig. 8).

In addition, experience concerning structural coupling and structures that trigger active oxidation is rather limited. Therefore, experimental investigations and modeling must be extended to elementary structural elements.

Summary

New numerical and measurement techniques to characterize both catalytic and oxidation behavior of TPS materials were presented. The hysteresis of SiC oxidation behavior with respect to PAT and vice versa has been explained theoretically. The theoretical model accounting for catalysis and oxidation behavior has been implemented in the advanced nonequilibrium Navier–Stokes code URANUS. Results for the highly dissociated flow around the MIRKA capsule show strong interaction between catalytic and other reactive processes. Radiation adiabatic surface temperatures have been found to be 120 K higher for active oxidation conditions as compared to passive oxidation conditions that depend mainly on atomic nitrogen recombination.

Results of exemplarily shown measurement campaigns feature particular characteristics such as the difference in temperature increase and erosion rate in air and oxygen plasmas. On the basis of surface reaction considerations, these features could be explained by the significance of atomic nitrogen recombination within air plasmas. In addition, these results are confirmed by further analytical and experimental investigations in Ref. 11. In a further step, emission spectroscopic measurements in the boundary layer were made. The expected erosion products and a release of Si with PAT could be detected that can be explained by the dissociation of erosion products in the hot boundary layer close to the surface. However, the spectroscopic investigation still lacks systematic investigations with respect to further species such as CO.

Acknowledgments

Many thanks go to DLR for the financial support within the German research program ASTRA under Contract FKZ 50 JR 0120. Thanks go to DLR, German Aerospace Research Institute, Stuttgart, and MAN Technologie for fruitful cooperation within ASTRA. Many thanks for financial support to Deutsche

Forschungsgemeinschaft (DFG) within the collaborative research center 259 "Hochtemperaturprobleme Rüchkkehrfähiger Raumtransportsysteme." Many thanks to DFG for supporting the development activities for the inductively heated plasma generators of IRS under Reference Au 85/15-1. The authors thank all members of the group who helped to perform the described measurement campaigns.

References

[1]Auweter-Kurtz, M., Fertig, M., Herdrich, G., Laux, T., Schöttle, U., Wegmann, T., and Winter, M., "Entry Experiments at IRS In-Flight Measurement During Atmospheric Entries," *Space Technology*, Vol. 23, No. 4, 2003, pp. 217–234.

[2]Hald, H., and Winkelmann, P., "Post Mission Analysis of the Heat Shield Experiment CETEX for the EXPRESS Capsule," International Astronautical Federation, Paper IAF-97-I.4.01, Oct. 1997.

[3]Ogasawara, K., Fujii, K., and Morito, T., "Aerothermodynamic Flight Experience in OREX and HYFLEX," 1st International Symposium on Atmospheric Reentry Vehicles and Systems, Association Aeronautique et Aerospatiale Française, Arcachon, France, March 1999.

[4]Herdrich, G., Auweter-Kurtz, M., and Habiger, H., "Pyrometric Temperature Measurements on Thermal Protection Systems," *Zeitschrift für Angewandte Mathematik und Mechanik*, Vol. 79, Supplement 3, 1999, pp. S945, S946.

[5]Hilfer, G., "Experimentelle und theoretische Beiträge zur Plasma-Wand-Wechselwirkung keramischer Hitzeschutzmaterialien unter Wiedereintrittsbedingungen," Ph.D. Dissertation, Inst. für Raumfahrtsysteme, Univ. of Stuttgart, Stuttgart, Germany, March 2000.

[6]Dabala, P., "Massenspektrometrische Untersuchungen zum Erosionsverhalten von Hitzeschutzmaterialien für Wiedereintrittsflugkörper," Ph.D. Dissertation, Inst. für Raumfahrtsysteme, Univ. of Stuttgart, Stuttgart, Germany, 2002.

[7]Heuer, A. H., and Lou, V. L. K., "Volatility Diagrams for Silica, Silicon Nitride, and Silicon Carbide and Their Application to High-Temperature Decomposition and Oxidation," *Journal of the American Ceramic Society*, Vol. 73, No. 10, 1990, pp. 2789–2803.

[8]Fertig, M., Frühauf, H.-H., and Auweter-Kurtz, M., "Modelling of Reactive Processes at SiC-Surfaces in Rarefied Nonequilibrium Airflows," AIAA Paper 2002-3102, June 2002.

[9]Herdrich, G., Auweter-Kurtz, M., Kurtz, H. L., Laux, T., and Winter, M., "Operational Behavior of the Inductively Heated Plasma Source IPG3 for Reentry Simulations," *Journal of Thermophysics and Heat Transfer*, Vol. 16, No. 3, 2002, pp. 440–449.

[10]Laux, T., and Auweter-Kurtz, M., "Untersuchung des Passiv-Aktiv-Übergangs an SiC in Sauerstoffplasmen," Deutsche Gesellschaft für Luft- und Raumfahrt–Jahrestagung, Paper DGLR-JT2000-207, Leipzig, Germany, Sept. 2000.

[11]Laux, T., "Untersuchung zur Hochtemperaturoxidation von Siliziumkarbid in Plasmaströmungen," Ph.D. Dissertation, Inst. für Raumfahrtsysteme, Univ. of Stuttgart, Stuttgart, Germany, July 2004.

[12]Pidan, S., Auweter-Kurtz, M., Herdrich, G., and Fertig, M., "Determination of Recombination Coefficients and Spectral Emissivity of Thermal Protection Materials," AIAA Paper 2004-2274, June–July 2004.

[13]Wagner, C., "Passivity During the Oxidation of Silicon at Elevated Temperatures," *Journal of Applied Physics*, Vol. 29, No. 9, 1958, pp. 1295–1297.

[14]Turkdogan, E. T., Grieveson, P., and Darken, L. S., "Enhancement of Diffusion-Limited Rates of Vaporization of Metals," *Journal of Physical Chemistry*, Vol. 67, No. 8, 1963, pp. 1647–1654.

[15]Pretorius, R., Strydom, W., and Mayer, J. W., "Si Tracer Studies of the Oxidation of Si, $CoSi^2$ and PtSi," *Physical Review B: Solid State*, Vol. 22, No. 4, 1980, pp. 1885–1891.

[16]Stewart, D. A., "Determination of Surface Catalytic Efficiency for Thermal Protection Materials—Room Temperature to Their Upper Use Limit," AIAA Paper 96-1863, June 1996.

[17]Rosner, D. E., and Allendorf, H. D., "High Temperature Kinetics of the Oxidation and Nitridation of Pyrolytic Silicon Carbide in Dissociated Gases," *Journal of Physical Chemistry*, Vol. 74, No. 9, 1970, pp. 1829–1839.

[18]Fertig, M., and Frühauf, H.-H., "Detailed Computation of the Aerothermodynamic Loads of the MIRKA-Capsule," *Proceedings of the Third European-Symposium on Aerothermo-Dynamics for Space Vehicles*, European Research and Technology Centre, Noordwijk, The Netherlands, 1999, pp. 703–710.

[19]Aldinger, F., Auweter-Kurtz, M., Fertig, M., Herdrich, G., Hirsch, K., Lindner, P., Matusch, D., Neuer, G., Schumacher, U., and Winter, M., "Behavior of Reusable Heat Shield Materials Under Re-Entry Conditions," *Basic Research and Technologies for Two Stage to Orbit Vehicles*, edited by G. Sachs, S. Wagner, and D. Jacob, Wiley-VCH, Weinheim, Germany, 2005.

[20]Röck, W., "Simulation des Eintritts einer Sonde in die Atmosphäre des Saturnmondes Titan in einem Plasmawindkanal," Ph.D. Dissertation, Inst. für Raumfahrtsysteme, Univ. of Stuttgart, Stuttgart, Germany, Dec. 1998.

[21]Auweter-Kurtz, M., Fertig, M., Herdrich, G., Pidan, S., and Winter, M., "Advanced In-Flight Sensor Systems for Atmospheric Entry Maneuvres," AIAA Paper 2004-2169, June–July 2004.

[22]Herdrich, G., Löhle, S., Auweter-Kurtz, M., Endlich, P., Fertig, M., Pidan, S., and Schrejber, E., "IRS Ground-Testing Facilities: Thermal Protection System Development, Code Validation and Flight Experiment Development," AIAA Paper 2004-2596, June–July 2004.

T. Lin
Associate Editor